Formation of Hirano bodies in *Dictyostelium* and mammalian cells induced by expression of a modified form of an actin-crosslinking protein

Andrew G. Maselli, Richard Davis, Ruth Furukawa and Marcus Fechheimer*

Department of Cellular Biology, University of Georgia, Athens, Georgia 30602, USA

*Author for correspondence (e-mail: fechheim@cb.uga.edu)

Accepted 26 February 2002

Journal of Cell Science 115, 1939-1952 (2002) © The Company of Biologists Ltd

Summary

We report the serendipitous development of the first cultured cell models of Hirano bodies. Myc-epitope-tagged forms of the 34 kDa actin bundling protein (amino acids 1-295) and the CT fragment (amino acids 124-295) of the 34 kDa protein that exhibits activated actin binding and calcium-insensitive actin filament crosslinking activity were expressed in *Dictyostelium* and mammalian cells to assess the behavior of these modified forms in vivo. *Dictyostelium* cells expressing the CT-myc fragment: (1) form ellipsoidal regions that contain ordered assemblies of F-actin, CT-myc, myosin II, cofilin and α-actinin; (2) grow and develop more slowly than wildtype, but produce normal morphogenetic structures; (3) perform pinocytosis and phagocytosis normally; and (4) produce a level of total actin equivalent to wildtype, but a higher level of F-actin. The paracrystalline inclusions bear a striking resemblance to Hirano bodies, which are associated with a number of pathological conditions. Furthermore, expression of the CT fragment in murine L cells results in F-actin rearrangements characterized by loss of stress fibers, accumulation of numerous punctate foci, and large perinuclear aggregates, the Hirano bodies. Thus, failure to regulate the activity and/or affinity of an actin crosslinking protein can provide a signal for formation of Hirano bodies. More generally, formation of Hirano bodies is a cellular response to or a consequence of aberrant function of the actin cytoskeleton. The results reveal that formation of Hirano bodies is not necessarily related to cell death. These cultured cell models should facilitate studies of the biochemistry, genetics and physiological effects of Hirano bodies.

Key words: Cytoskeleton, Actin-binding protein, *Dictyostelium*, Hirano body, Neurodegeneration

Introduction

Abnormal protein aggregation results in formation of distinct types of protein assemblies frequently associated with disease. For example, neurodegenerative diseases are associated with deposition of peptides derived from β-amyloid precursor protein (β-APP) in senile plaques (Mattson, 1997; Selkoe, 1998), tau protein in neurofibrillary tangles (Goedert, 1999; Tolnay and Probst, 1999), α-synuclein in Lewy bodies (Galvin et al., 1999; Goedert, 1999; Papka et al., 1998), and proteins with polyglutamine repeats in insoluble aggregates (Lunkes et al., 1998; Paulson, 2000). Insoluble aggregates containing misfolded proteins in β-sheet structures underlie a variety of diseases classified as amyloidoses that are not specific to the nervous system (Buxbaum and Tagoe, 2000; Koo et al., 1999). Furthermore, misfolded proteins collect in structures termed aggresomes that can be induced either by expression of misfolded proteins or inhibition of the proteasome (Garcia-Mata et al., 1999; Johnston et al., 1998; Wigley et al., 1999).

Cytoplasmic inclusions termed Hirano bodies have been described in a variety of neurodegenerative diseases and other conditions that produce persistent injury or stress (Hirano, 1994). The structures contain actin filaments and actin-associated proteins (Galloway et al., 1987; Goldman, 1983; Maciver and Harrington, 1995). However, their mechanism of formation, composition and relation to disease remains poorly understood.

In this study, we report the serendipitous development of a cultured cell model for studies of Hirano bodies in the cellular slime mold *Dictyostelium discoideum*, a lower eukaryote with a well-characterized cytoskeleton, and facile methods for protein expression and creation of mutant strains (Mann et al., 1998; Noegel and Schleicher, 2000). The 34 kDa protein is one of 11 actin crosslinking proteins present in *Dictyostelium* (Furukawa and Fechheimer, 1997). In vitro studies reveal that actin bundling by the purified 34 kDa protein is calcium regulated (Fechheimer, 1987; Fechheimer and Furukawa, 1993; Fechheimer and Taylor, 1984; Lim and Fechheimer, 1997). Experiments with defined segments of recombinant protein reveal three actin-binding sites located at amino acids 1-123, 193-254 and 279-295 (Lim et al., 1999a). The strongest of these sites, located at amino acids 193-254, is necessary and sufficient for co-sedimentation with F-actin in vitro (Lim et al., 1999a). The CT fragment, comprising amino acids 124-295, lacks the inhibitory domain located in the N-terminus that modulates the activity of the strong actin-binding site through an intramolecular interaction (Lim et al., 1999b). Truncation of the inhibitory region from the CT fragment results in enhanced binding and crosslinking of actin filaments that is calcium-insensitive (Lim et al., 1999b).

In this paper, we report that expression of low levels of the CT protein in *Dictyostelium* induces formation of paracrystalline actin inclusions that resemble Hirano bodies in both ultrastructure and composition as assessed by immunocytochemistry. Similarly, expression of the CT fragment induces formation of Hirano bodies in murine L cells. These results show that formation of Hirano bodies is restricted neither to mammalian cells nor to nerve cells. Rather, the formation of Hirano bodies appears to be a general response to or consequence of aberrant function of the actin cytoskeleton. In addition, we report the first studies of the physiological effects of Hirano bodies on cell function.

Materials and Methods

Vector construction

Vectors for expression in *Dictyostelium* were made from pBORP (Ostrow et al., 1994), which has an ampicillin-resistance gene, bacterial origin of replication, a G418 resistance cassette, and an actin 15 promoter and actin 8 terminator flanking a *Bam*HI restriction enzyme site used for insertion of protein sequences to be expressed. The 34 kDa-myc* and CT-myc† expression vectors were constructed in pBORP using cloned cDNA encoding the 34 kDa protein (Fechheimer et al., 1991), and custom oligonucleotides to introduce the MYC epitope, to prime the PCR and to introduce *Bam*HI restriction sites. The CT-myc vector contains a deletion of a single adenosine in the sixth codon of CT-myc (codon 128 of full-length 34 kDa protein) resulting in a frame shift and premature termination of protein translation at codon 8 of CT-myc (codon 130 of full-length 34 kDa protein). Translation was probably alternatively initiated at low efficiency at the adjacent ATG codon 7 of CT-Myc (codon 129 of full-length 34 kDa protein) resulting in low expression levels of the CT-myc protein in *Dictyostelium* (Fig. 1C).

Growth and transformation of *Dictyostelium*

AX-2 and derivatives described below were routinely maintained in axenic shaking cultures in HL-5 media (Loomis, 1971). Cell transformation was performed and growth rates were measured as described previously (Rivero et al., 1996). Clones were screened by western blotting or staining with rhodamine-labelled phalloidin to identify actin inclusions. Once a clone was established, it was transferred to shaking culture in HL-5 medium, and multiple aliquots were frozen at –80°C in HL-5 media supplemented with 10% DMSO. Since the incidence of actin inclusions decreased during routine passage of cells, all assays were performed on cells that were maintained in shaking culture for less than 30 days.

Development and germination

Cells were grown in HL-5 media in suspension to a concentration of 3×10^6 cells/ml, harvested by centrifugation, washed once in 17 mM Soerensen buffer, and 1×10^7 cells in 0.5 ml 17 mM Soerensen phosphate buffer were plated on 100 mm non-nutrient agar plates. Photographs were taken on a Wild 500 MacroScope.

To assess germination of spores, fruiting bodies were collected and the spores were placed in HL-5 media. The number of amoebae and ungerminated spores were counted after 4.5 hours to assess viability. The amoebae germinated from spores were stained with rhodamine-labeled phalloidin to identify actin inclusions.

*Full-length *Dictyostelium* 34 kDa actin-bundling protein (amino acids 1-295) with a C-terminal myc epitope tag.
†C-terminal portion of the *Dictyostelium* 34 kDa actin-bundling protein (amino acids 124-295) with a C-terminal myc epitope tag.

Electron microscopy

Dictyostelium cells were fixed for transmission electron microscopy as described previously (Novak et al., 1995). Cells were embedded in EPON 812 and sectioned on an RMC 5000 ultramicrotome (Tuscon, AZ) with a diamond knife. Micrographs were taken on a Phillips 400 TEM.

Immunofluorescence

Dictyostelium cells were fixed for 20 minutes in 3.7% formaldehyde in 17 mM phosphate buffer containing 1 mM $CaCl_2$, pH 7.1, and permeabilized using acetone at –20°C for 2 minutes as described previously (Fechheimer, 1987). Cells were stained with B2C monoclonal antibody to the 34 kDa protein (Furukawa et al., 1992) or anti-myc monoclonal antibody 9E10 (ATCC CRL-1729). Tubulin and *Dictyostelium* MAP were identified with rat monoclonal antibody YL 1/2 and antibody AX3, respectively (gift of M. Kimble, University of South Florida). Myosin II was identified with mouse polyclonal antibody NU48 (gift of R. Chisholm, Northwestern University Medical School). Myosin II heavy chain was identified with polyclonal antibody 9555-3 (gift of A. De Lozanne, University of Texas at Austin). Cofilin was identified with rabbit polyclonal antibody (gift of H. Aizawa, Tokyo Metropolitan Institute of Medical Science, and C. Chia, University of Nebraska). EF-1α, cofilin, ABP120 and α-actinin were identified with rabbit polyclonal antibodies (gift of J. Condeelis, Albert Einstein College of Medicine). The rhodamine- and fluorescein-conjugated secondary antibodies were obtained from Sigma Chemical Co. (St Louis, MO). The rhodamine- and Oregon green 488-labelled phalloidins were obtained from Molecular Probes (Eugene, OR).

Phagocytosis and pinocytosis

The phagocytosis assay was performed with fluorescently labeled yeast in suspension essentially as described previously (Maniak et al., 1995) and modified by Meg Titus (University of Minnesota). The pinocytosis assay was performed using lucifer yellow on cells attached to 24-well tissue culture plates as described (Rivero et al., 1996).

Measurements of actin in *Dictyostelium* amoebae

The total actin content of the amoebae was assessed by western blotting. *Dictyostelium* cells were counted, washed and lysed, and proteins were resolved by SDS-PAGE. The samples were then blotted to nitrocellulose, labeled with an anti-actin monoclonal primary antibody (10-B-3, gift of M. Kandasamy and R. B. Meagher, University of Georgia) followed by an alkaline-phosphatase-conjugated secondary antibody (Promega, Madison, WI), and treated with BCIP/NBT to visualize the bands. The blot was photographed with direct positive black and white film, and scanned using a Molecular Dynamics Laser Scanning Densitometer.

F-actin levels for the whole population of cells were determined with rhodamine-labelled phalloidin (Sigma, St. Louis, MO) using the method described previously (Cano et al., 1992). Data presented represent fluorescence units per mg total protein from six independent samples.

Comparisons of the amount of F-actin in single cells were made by measurement of the fluorescence from single cells stained with rhodamine-labelled phalloidin. Images were recorded with a Mighty Max Cooled CCD camera (Princeton, Trenton, NJ). Care was taken not to saturate any pixels in the array. The mean pixel intensity of AX-2 and CT-myc cells were compared using IP lab image analysis software (Scanalytics, Fairfax, VA). The data reported represent mean pixel values from at least 24 individual cells.

Expression of CT fragment in murine L cells

The sequences encoding the CT fragment of the 34 kDa protein (aa

124-295) were subcloned into the *Bam*HI site of the vector pEGFP N1 (Clontech) following amplification by PCR using custom oligonucleotides. The vector was designed to express the CT fragment alone, and not a fusion protein of CT with GFP. The coding sequence was confirmed by automated DNA sequencing.

L-cell fibroblasts were maintained in RPMI-1640 supplemented with 15% bovine serum, 100 U/ml penicillin/streptomycin, and 2 mM L-glutamine at 37°C in 5% CO_2. The cells were plated at 1×10^5 cells/22 mm^2 coverslip (50-60% confluence), and transfected using Lipofectamine Plus (Life Technologies) according to the manufacturer's protocol. Cells were transfected with no DNA (mock), or 1 μg of the pEGFP vector only or the pCTEGFP plasmid. The transfection efficiency was approximately 60% as assessed from the expression of GFP in the cells transfected with vector alone.

Cells were fixed 24 hours following replacement of complete media to the transfected cells. Coverslips were rinsed in PBS, transferred to 3.7% formaldehyde in PBS for 25 minutes, washed briefly three times in PBS, permeabilized in 0.1% Triton X-100 in PBS for 5 minutes, washed briefly three times in PBS, blocked in 1% BSA in PBS for 1 hour, and stained with Oregon Green 488-labelled phalloidin for 1 hour (Molecular Probes) before being mounted.

All slides were coded and scored by observers unbiased by knowledge of the identity of the treatment groups. Cells were counted and categorized according to the F-actin distribution as follows: (1) predominantly in cortical arrays, stress fibers, and filament bundles; (2) predominantly in punctate and stellar foci; and 3) contain a large aggregate/Hirano body. All experiments were repeated at least 3 times. Significance was judged using a Student's T test to compare the means ± standard deviations of the control and CT expressing cells.

Results

Expression of full-length and truncated 34 kDa proteins in *Dictyostelium*

Myc epitope-tagged recombinant proteins were expressed in the wild-type *Dictyostelium* axenic cell line AX-2. The level of recombinant protein production was assayed by western blotting of cell lysates using antibodies to the native 34 kDa protein (Fig. 1A), and the myc epitope tag (Fig. 1B). The full-length 34 kDa protein, with a C-terminal myc tag (34 kDa-myc protein), is expressed at a level equivalent to or slightly higher than the endogenous 34 kDa protein (Fig. 1A). The N-terminal truncation fragment CT-myc is expressed at a low level that is less than 10% of the endogenous 34 kDa protein (Fig. 1A,B). The low level of expression of CT-myc is the fortuitous result of a frame shift in the coding sequence. A single base deletion causes a frame shift and a new stop codon so that the protein produced is most likely the result of initiation at a nearby alternate methionine (Fig. 1C). When a CT-myc vector without the frame shift was constructed, no clones expressing CT-myc protein could be isolated, which suggests that cells expressing higher levels of the CT-myc protein are not viable.

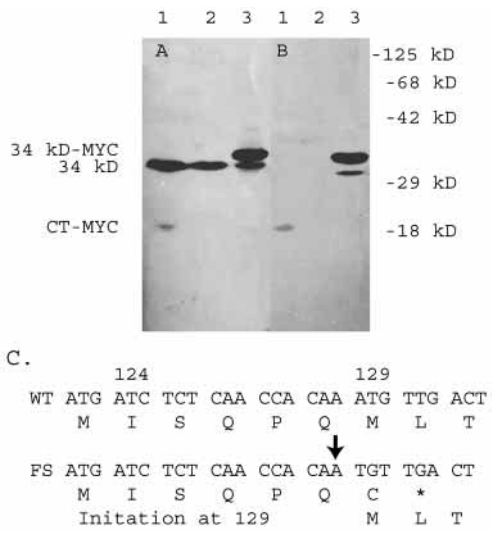

Fig. 1. Expression of full-length 34 kDa-myc and CT-myc proteins in *Dictyostelium*. (A,B) Lysates of CT-myc expressing cells (lane 1), wild-type AX-2 (lane 2), and cells expressing full-length 34 kDa-myc (lane 3) were resolved by SDS-PAGE, blotted to nitrocellulose, and probed with monoclonal antibody B2C, which is reactive to native 34 kDa protein (A), or monoclonal antibody 9E10, which is reactive to the myc epitope tag (B). Note that 34 kDa-myc and CT-myc proteins are expressed at levels roughly equivalent to and significantly less than the endogenous 34 kDa protein, respectively. (C) Nucleotide and amino acid sequence at the translational start site of the CT protein. The wild-type sequence (WT), the frame shift (FS) resulting from deletion of an adenosine (arrow), and the alternative ATG methionine codon presumed to initiate synthesis of the CT-myc protein are shown.

CT-myc induces formation of actin-containing ellipsoids

In cells expressing full-length 34 kDa-myc protein, the localization of the full-length 34 kDa protein with the myc epitope tag is identical to the localization pattern for the native 34 kDa protein. Both native and tagged proteins can be found in the leading edge and the cell cortex of vegetative amoebae (Fig. 2). The actin localization pattern in cells expressing 34 kDa-myc protein is the same as AX-2 wild-type cells, and largely overlaps the localization of the 34 kDa protein.

Surprisingly, cells expressing low levels of the CT-myc protein produce ellipsoidal inclusions that label strongly with rhodamine-labelled phalloidin, anti-34-kDa protein antibody (B2C), and anti-myc antibody (Figs 2, 3). The B2C monoclonal antibody to the 34 kDa protein recognizes an epitope within the CT fragment, and so is expected to label the expressed CT-myc (R. W. L. Lim, R.F. and M.F., unpublished). The ellipsoids do not incorporate all the endogenous full-length 34 kDa protein, as cells containing ellipsoids exhibit significant staining for the 34 kDa protein in the cortex. By contrast, staining of the cortex with the antibody to the myc epitope is less prominent, which indicates that the cortical staining emanates primarily from full-length endogenous 34 kDa protein. The difference in localization is apparent in a direct comparison of the anti-34-kDa protein and anti-myc antibodies (Fig. 3). The B2C antibody staining of both the native 34 kDa protein and the CT-myc protein is visible in both the cell cortex, the normal site of localization and the ellipsoid. By contrast, the actin-containing ellipsoid is stained predominantly when the cells are labeled with antibody to the myc epitope. Although the ellipsoid is roughly the same size as the nucleus, DAPI staining of DNA demonstrates that the ellipsoids are distinct from the nucleus (data not shown).

CT-myc cells were labeled with a variety of antibodies to assess the status of selected known cytoskeletal proteins. The ellipsoids do not contain α-tubulin or a *Dictyostelium* MAP

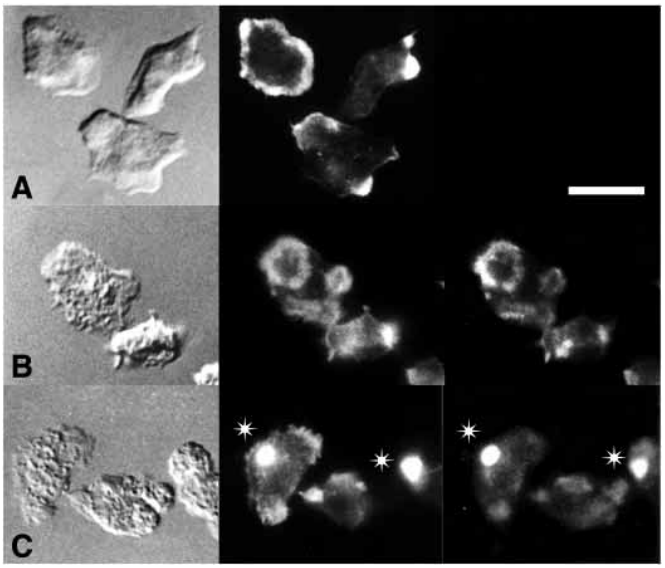

Fig. 2. Intracellular localization of F-actin and myc epitope in wild-type cells, and cells expressing 34 kDa-myc and CT-myc proteins. Wild-type AX-2 (A), 34 kDa-myc- (B) and CT-myc (C)-expressing cells were observed by DIC (left), and stained with rhodamine-labelled phalloidin (middle) and antibody to the myc-epitope tag (right). There is extensive cortical staining of F-actin in the AX-2 and 34 kDa-myc cells (A,B). By contrast, the CT-myc cells reveal ellipsoids that label strongly for actin and for the myc epitope (C). The asterisks indicate the ellipsoids. Bar, 10 μm.

(Kimble et al., 1992), and no differences in the pattern of interphase microtubules between wild-type cells and cells expressing CT-myc are detected (Fig. 4A). The ellipsoids are also enriched in myosin II, cofilin and α-actinin (Fig. 4B-D), but do not stain with antibodies to EF-1α, ABP 120 (Fig. 4E,F), and myosin I (data not shown).

Ultrastructure and actin filament organization in the ellipsoids

Ultrastructural observation reveals that the ellipsoids are present in the cytoplasm of CT-myc cells, and that no lipid bilayer circumscribes the ellipsoids (Fig. 5A). The ellipsoids are most commonly located near the center of the cell, but they also can be observed adjacent to the cell membrane.

The F-actin in the ellipsoids is highly ordered, as revealed by transmission electron microscope images of thin sections. An oblique section through the ellipsoids reveals a pattern that resembles a herringbone fabric (Fig. 5B). Tilting the section reveals that the herringbone appearance is a plane of section effect, as the same field reveals parallel filaments when viewed at a 45° tilt (Fig. 5C). This observation is confirmed by cross-sections that reveal different degrees of order in the ellipsoids. Some of the regions have an appearance similar to cytoplasmic extensions that can be seen at the cell periphery, and presumably contain loosely ordered actin that is not well preserved using methods of preparation for electron microscopy that include treatment with OsO_4 (Maupin-Szamier and Pollard, 1978) (Figs 5, 6). Many regions are highly ordered, with the filaments arranged in a square packed arrangement (Fig. 6A,D). In these square packed regions the

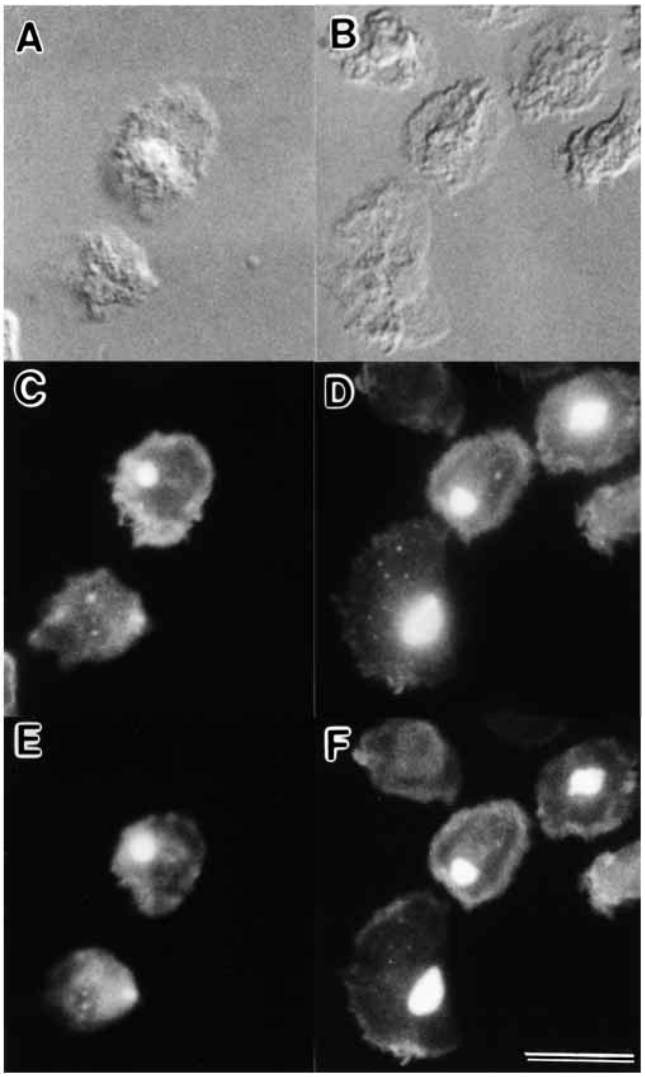

Fig. 3. Intracellular localization of F-actin, 34 kDa protein, and myc epitope tag in CT-myc cells. CT-myc cells were viewed by DIC microscopy (A,B), stained with phalloidin to localize F-actin (C,D), and stained with antibody to localize the 34 kDa protein (F), or myc epitope tag (E). F-actin and the 34 kDa protein epitopes are present in both the ellipsoids and the cortical regions of the CT-myc cells. By contrast, the myc epitope is largely confined to the ellipsoids in CT-myc cells. Bar, 10 μm.

filaments are arranged in a double row, with a center to center spacing of 20 nm, separated by a space of 25 nm between double rows. The pattern of double rows is clearly visible in both longitudinal and cross-sections (Fig. 6C,D). Square packed actin bundles have not been observed previously in *Dictyostelium*, but do form in vitro in mixtures of actin with *Dictyostelium* elongation factor 1α (ABP 50) (Owen et al., 1992). However, note that ABP-50 is not concentrated in these structures in vivo (Fig. 4F). Hexagonally ordered actin filaments represent the most compact state. In this arrangement each actin filament is 15 nm from its six nearest neighbors (Fig. 6B). In a fortuitous section these different states of order can be seen in the same ellipsoid (Fig. 6A), showing both the square packed and hexagonally packed filament patterns.

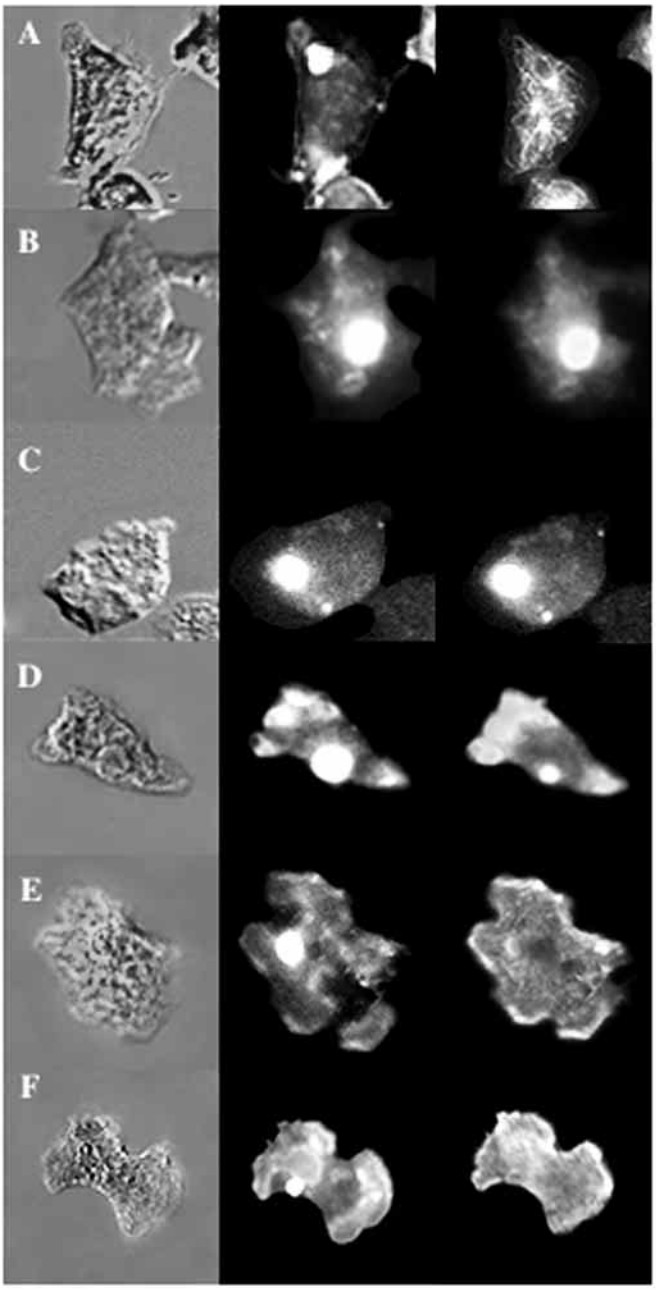

Fig. 4. Localization of tubulin, myosin, cofilin, α-actinin, ABP 120 and EF 1-α in CT-myc cells. In each set of images, the cells were viewed by DIC microscopy (left), stained with phalloidin to localize F-actin (middle), and stained with antibody to localize specific cytoskeletal proteins (right). (A) α-tubulin; (B) myosin II; (C) cofilin; (D) α-actinin; (E) ABP 120; (F) EF 1-α. The CT-myc-induced ellipsoids are enriched for actin, myosin II, cofilin and α-actinin, but not for α-tubulin, ABP 120, and EF-1α. Bar, 10 μm.

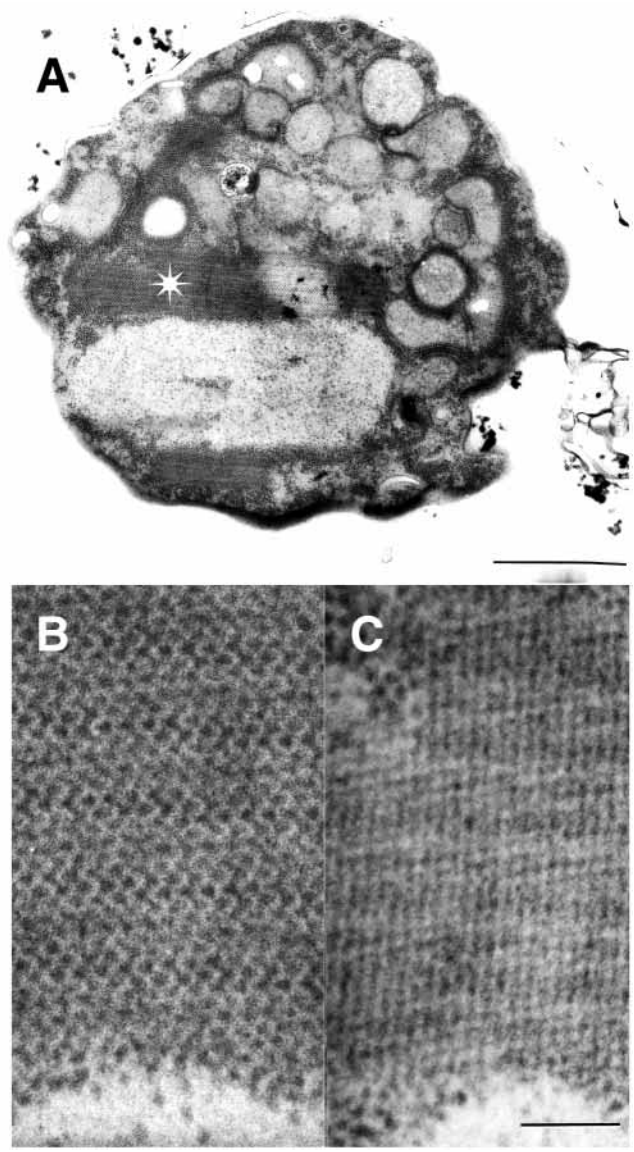

Fig. 5. Ultrastructure of the CT-myc induced ellipsoid. (A) Micrograph of CT-myc-expressing cell, with a large inclusion with herringbone pattern (bar, 1 μm). (B,C) High magnification tilt images of ellipsoid inclusion at 0° tilt and 45° tilt for panels B and C, respectively (bar, 10 nm). An asterisk marks the region in A that is shown in B and C.

Growth, development and endocytosis by CT-myc cells

Since the CT-myc cells reveal dramatic reorganization of F-actin, the ability of the cells to perform the primary functions of growth and development was assessed. CT-myc cells grow slowly in shaking axenic culture at 20°C. The G418-resistant AX-2 cells expressing vector alone double 2.06 times per day as opposed to 2.04 doubles per day for 34 kDa-myc cells and only 1.46 doubles per day for CT-myc cells. To track the portion of the population with ellipsoids, samples of CT-myc cells were taken daily and stained with rhodamine phalloidin. The number of cells presenting ellipsoids remained constant at about 40% until late log phase. During late log phase the number of ellipsoids visible in the population was substantially smaller. Furthermore, ellipsoids are rare in cells that have been maintained in culture for more than 1 month. Each of these observations was confirmed in at least two independent transformants, indicating that they are a consequence of expression of CT-myc, and not from adventitious effects arising from integration of the vector and selection of cell clones. Since loss of expression is an inevitable consequence of the slow growth of the CT-myc cells, new cultures were

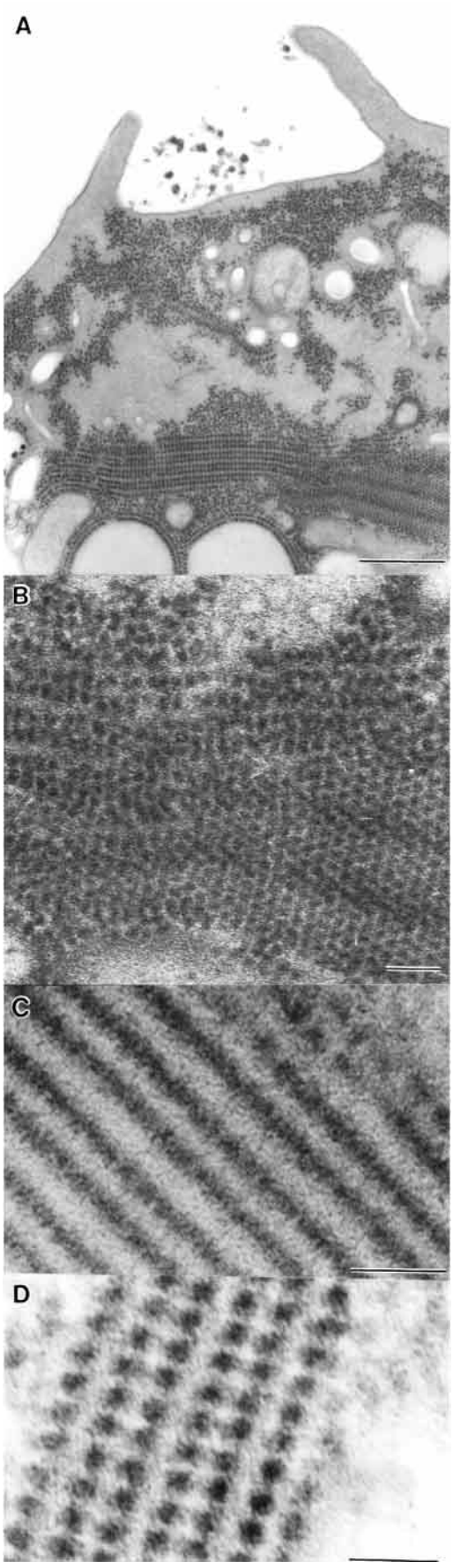

Fig. 6. Transverse and longitudinal sections reveal the organization of the actin filaments in ellipsoids of CT-myc cells. (A) Note regular inclusion in cytoplasm revealing square packed and hexagonally packed organizations. (B) Higher magnification of the lower right region of the ellipsoid in A. (C) Longitudinal section of 10 nm filaments in an inclusion. (D) Cross-section of square packed filaments. Bar, 0.5 μm (A); 0.1 μm (B); 50 nm (C,D).

regularly established from frozen stock, and all data presented are from cells maintained in axenic shaking culture for less than 30 days.

To assess the ability of CT-myc cells to undergo development, cells from shaking culture were collected and washed by centrifugation and plated on non-nutrient agar. The CT-myc cells are delayed in development by 3-6 hours (Fig. 7). When the wild-type and 34 kDa-myc expressing cells are making mounds, the CT-myc cells are only beginning to stream. When wild-type cells are beginning to culminate, the CT-myc cells have just started making mounds. After 30 hours, the CT-myc cells produce fruiting bodies with normal morphology, approximately 6 hours later than wild-type cells (Fig. 7).

The spores that are produced by CT-myc cells produce viable amoebae. After 4.5 hours in HL-5, 67% and 61% of the 34 kDa-myc and CT-myc spores germinated, respectively. The population of amoebae germinated from CT-myc spores contains about 40% individuals with large ellipsoids, a fraction similar to that of the population from which the spores were derived. Thus, the selection against CT-myc expression that was observed after long term culture was not evident after a single round of development and subsequent germination.

The presence of the 34 kDa protein and actin in the phagocytic cup (Furukawa et al., 1992; Furukawa and Fechheimer, 1994; Rezabek et al., 1997) and the participation of actin in macropinocytosis in *Dictyostelium* (Hacker et al., 1997) suggested that alteration of the actin cytoskeleton by expression of CT-myc might have a detrimental effect on endocytosis. Surprisingly, the rate of phagocytosis of fluorescently labeled yeast in shaking culture is not significantly different in assays using CT-myc and AX-2 cells (data not shown). Further, the rate of pinocytotic uptake of lucifer yellow by adherent cells in HL-5 axenic media reveals no significant difference between wild-type AX-2 and CT-myc cells (data not shown).

Changes in actin in CT-myc cells

The presence of stable F-actin-containing ellipsoids in the cytoplasm of *Dictyostelium* suggests that the actin levels and/or dynamics in the cell may be altered. Actin comprises 8% of the protein in axenic *Dictyostelium* amoebae (Brier et al., 1983). CT-myc cells had a level of total actin that was 96±23% of wild-type as assessed by western blots of whole cell lysates.

The total actin pool contains free G-actin, unpolymerized sequestered monomeric actin, and F-actin in quantities that depend on changes in actin-monomer-binding proteins, and the presence of free or capped barbed and pointed ends on the actin filaments (Fechheimer and Zigmond, 1993). The F-actin levels in the whole population were examined by lysing cells, labeling the F-actin with rhodamine-labeled phalloidin, and measuring bound phalloidin after high speed sedimentation of

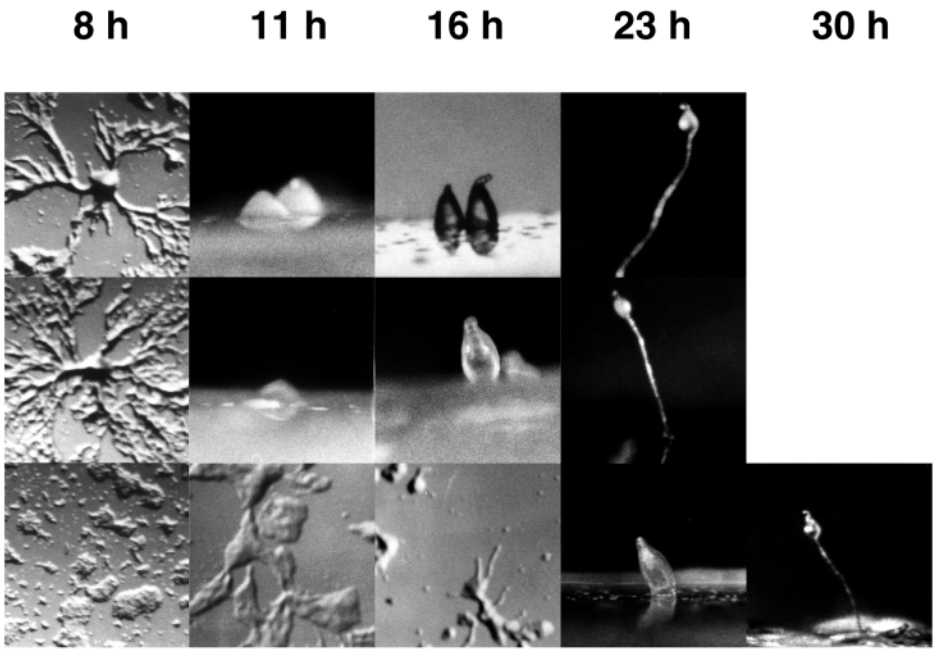

Fig. 7. Rate of development of wild-type AX-2 (top), 34 kDa-myc (middle), and CT-myc (bottom) cells. Note that CT-myc-expressing cells are delayed in development by 3-6 hours compared with wild-type and 34 kDa-myc cells.

the actin filaments. The F-actin levels in CT-myc cells are 120±13% of wild-type. This difference is not statistically significant. However, since only 40% of CT-myc cells contain ellipsoids, the difference in F-actin levels between wild-type and CT-myc cells with ellipsoids may be more striking than is revealed by measurements of the bulk population of CT-myc cells.

To compare F-actin levels between AX-2 and the subsets of CT-myc cells that do or do not contain ellipsoids, we examined the intensity of rhodamine-labelled, phalloidin-derived fluorescence from selected cells with images obtained and quantified using a cooled CCD camera. These comparisons were made by identifying rhodamine-labelled, phalloidin-stained CT-myc cells that did or did not exhibit ellipsoids, and comparing their mean pixel intensity with AX-2 cells. Cells in the CT-myc population that did not display ellipsoids had 117±3.8% of the F-actin of wild-type. The level of F-actin in CT-myc cells presenting ellipsoids was 183±4.6% of wild-type. Thus, the F-actin levels in CT-myc cells containing ellipsoids is significantly higher than that in wild-type cells. Since CT-myc cells contain equivalent total actin and increased F-actin compared with wild-type cells, these cells must have a smaller pool of unpolymerized actin than wild-type cells.

Formation of Hirano bodies in L cells

The actin distribution in murine L cells expressing the CT fragment was investigated to determine whether the results obtained in *Dictyostelium* might be extended to a mammalian cell culture system. Control (untransfected, mock transfected, or vector only transfected) fibroblasts have a typical F-actin distribution characterized by cortical filaments, filament bundles and few punctate foci (Fig. 8A). Cells expressing the CT fragment exhibited a loss of stress fibers and cortical F-actin, and accumulated multiple punctate foci (Fig. 8B) and large aggregates resembling Hirano bodies (Fig. 8C-E). These results were quantified revealing that the decrease in stress fibers, and accumulation of multiple foci and large aggregates are representative of the populations (Fig. 8F). The differences in actin distributions of control and CT-transfected cells were statistically significant as assessed by a Student's *t*-test ($P<0.01$).

Discussion

Actin-containing inclusions, Hirano bodies, have been observed in a variety of normal and abnormal human and animal cells in vivo (Hirano, 1994). There is extensive similarity between Hirano bodies and the CT-myc-containing inclusions that we have described in *Dictyostelium*. Both of these highly ordered structures present elliptical cross-sections and are rod or disc shaped depending on the overall length (Hirano, 1994; Hirano et al., 1968). In both structures the appearance and arrangement of filaments varies with the plane of section or tilt of the stage, but ranges from a herringbone pattern in oblique sections to paired sheets of filaments in transverse or longitudinal sections (Figs 5, 6) (Schochet and McCormick, 1972; Tomonaga, 1974). Both structures contain filaments of 9-12 nm diameter (Hirano et al., 1968; Izumiyama et al., 1991; Schochet et al., 1968). A broad range of spacing between filaments in Hirano bodies from different patients has been reported (Hirano et al., 1968; Izumiyama et al., 1991), and these values span the range of 20 nm that we observe. Both mammalian and *Dictyostelium* inclusions frequently reveal juxtaposition of ordered and disordered regions (Fig. 5) (Peterson et al., 1986). Both the instability of actin using preparative methods for electron microscopy that employ OsO_4 (Maupin-Szamier and Pollard, 1978; Tilney and Tilney, 1994), and the remarkable ultrastructural preservation of the actin in Hirano bodies have been noted previously (Peterson et al., 1986), indicating that the actin in these inclusions is quite different in nature and stability from other actin-containing structures in the cell. The observed filament diameter of 10 nm is consistent with binding of an actin-binding protein such as cofilin, which is known to complex with actin to form 100 Å diameter filaments (McGough et al., 1997). At the immunocytochemical level, both CT-myc induced ellipsoids and Hirano bodies contain actin, cofilin, and α-actinin, and lack tubulin (Fig. 4) (Galloway et al., 1987; Goldman, 1983; Maciver and Harrington, 1995). Furthermore, neurofilaments have never been described in *Dictyostelium*, and are almost certainly absent from the *Dictyostelium* inclusions. In agreement, it was found that only 4 of >500 monoclonal antibodies reactive with neurofilaments

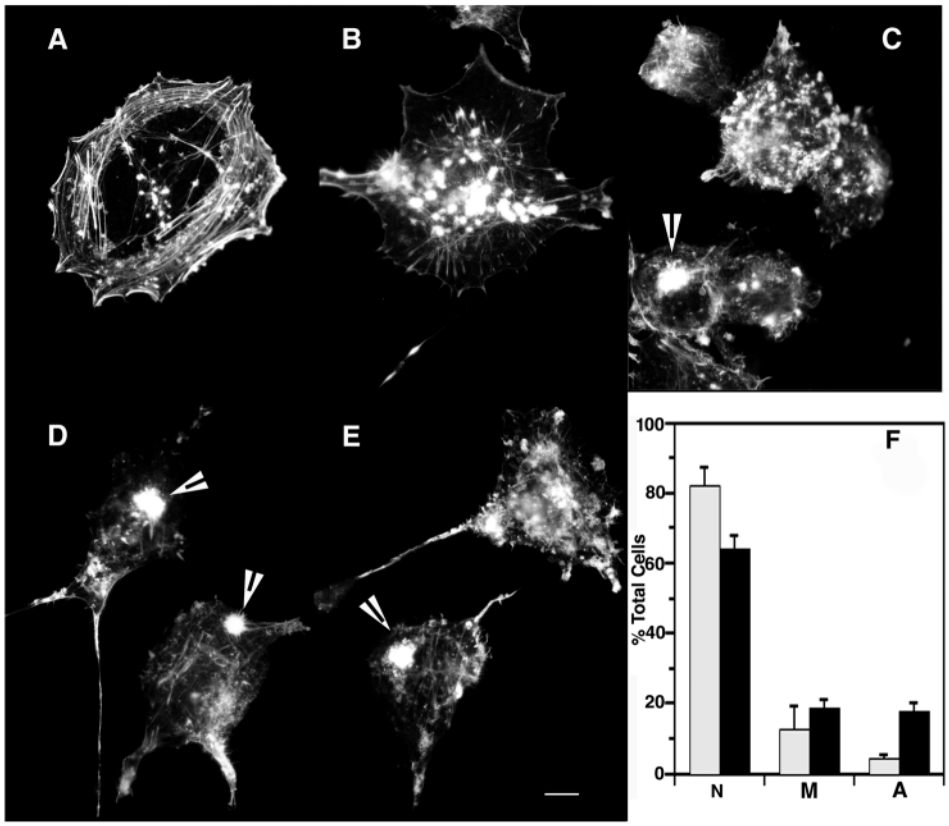

Fig. 8. Formation of Hirano Bodies in L cells expressing the CT Fragment. The distribution of F-actin was determined by staining with oregon green 488-labelled phalloidin as described in Materials and Methods. (A) Cortical actin, stress fibers and few punctate foci characterize the distribution of actin filaments in control cells. (B) Cells transfected with CT fragment exhibit loss of stress fibers and accumulation of punctate F-actin foci. (C-E) Some cells transfected with CT exhibit large elliptical inclusions highly enriched in F-actin that resemble Hirano bodies (marked with arrowheads) (bar, 10 μm). (F) L cells were mock transfected (gray bars) and CT transfected (black bars) and scored for F-actin distribution as: normal (N), most of the actin in cortical arrays and stress fibers; multiple foci (M), most of the F-actin in multiple punctate foci; aggregate (A), contain a large elliptical aggregate resembling a Hirano body. Results are shown as the mean±s.e.m. of six counts from three independent transfections of mock and CT cells. The CT-transfected cells have fewer and less prominent stress fibers and accumulate multiple foci and large aggregates of F-actin.

were reactive with hippocampal Hirano bodies (Schmidt et al., 1989). This striking similarity in the ultrastructure and composition of these structures is unmistakable, and supports the designation of the CT-myc inclusions described here as *Dictyostelium* Hirano bodies. Furthermore, the formation of large elliptical F-actin aggregates following expression of the CT fragment in L cells demonstrates that mammalian cultured cell models can also be exploited for studies of the dynamics and physiological significance of Hirano bodies (Fig. 8).

Hirano bodies have been reported in normal and pathological specimens from humans and animals providing our primary clues to their etiology. Hirano bodies form in association with a broad array of conditions including Alzheimer's disease (Gibson and Tomlinson, 1977; Mitake et al., 1997; Mori et al., 1986; Schmidt et al., 1989), Parkinson's disease (Hirano et al., 1968), Pick's disease (Schochet et al., 1968), amyotrophic lateral sclerosis (Hirano et al., 1968), ataxic Creutzfeldt-Jakob disease (Cartier et al., 1985), kuru (Field et al., 1969), scrapie (Field and Narang, 1972), Papovavirus (Hadfield et al., 1974), chronic alcoholism (Lass and Hagel, 1994), diabetes (Sima and Hinton, 1983), cancer (Fu et al., 1975; Gessaga and Anzil, 1975), muscle degeneration (Fisher et al., 1972), and neuronal degeneration associated with abnormal copper homeostasis (Anzil et al., 1974; Nagara et al., 1980; Peterson et al., 1986; Waggoner et al., 1999).

Hirano bodies have been observed most frequently in the hippocampus (Cartier et al., 1985; Gibson and Tomlinson, 1977; Hirano et al., 1968; Mitake et al., 1997; Mori et al., 1986; Ogata et al., 1972; Schmidt et al., 1989; Schochet et al., 1968), but have also been observed in other regions of the brain including Purkinje cells (Yamamoto and Hirano, 1985), cerebellum (Nagara et al., 1980; Peterson et al., 1986), cerebral cortex (Anzil et al., 1974), and peripheral neurons (Atsumi et al., 1980; Doering and Aguayo, 1987; Sima and Hinton, 1983; Yagishita et al., 1979). Hirano bodies are not restricted to neurons; they have been reported in oligodendroglial cells (Gibson, 1978; Okamoto et al., 1982; Sima and Hinton, 1983), muscle fibers (Fernandez et al., 1999; Fisher et al., 1972; Tomonaga, 1983), and testis (Setoguti et al., 1974).

These findings have supported a variety of suggestions regarding the physiological or pathological significance of Hirano bodies. Because Hirano bodies were reported in brain tissue from individuals with a wide variety of conditions, they have been characterized as a nonspecific manifestation of neuronal degeneration (Schochet and McCormick, 1972), nonspecific changes with no relation to pathology (Ogata et al., 1972), and nonspecific arrangements of filament units largely devoid of cytopathological significance (Gessaga and Anzil, 1975). However, both the data in the literature and our results presented above support a broader interpretation. Since the filament arrangement is paracrystalline and highly ordered and contains actin but neither microtubules nor intermediate filaments, the claim that Hirano bodies are a nonspecific arrangement of filaments is clearly not well supported. Moreover, the finding of Hirano bodies in a variety of tissues and in association with a broad array of conditions does not prove that they are nonspecific and lacking in cytopathological significance. Rather, we propose that a range of conditions may generate a signal(s) that causes rearrangement of the actin cytoskeleton and induces the formation of Hirano bodies. Our finding that Hirano bodies can be induced to form by

expression of an activated and unregulated fragment of an actin crosslinking protein strongly supports this interpretation.

It is interesting to ponder the mechanism of formation of the Hirano bodies. First, the CT fragment binds with high affinity to actin filaments in vitro, and would disassociate slowly from actin filaments strongly delaying their disassembly (Zigmond et al., 1992). The CT fragment induces formation of large extended tangles of actin filaments in vitro (Lim et al., 1999a; Lim et al., 1999b). This could result in accumulation of ordered structures, promoted by entropic forces that would induce alignment into a highly ordered stable array (Furukawa and Fechheimer, 1997). Second, the presence of myosin II in the Hirano bodies (Fig. 4B) raises the possibility that active generation of contractile force is involved in the formation of these structures. Third, it is possible that following initial formation of a number of small arrays, formation of a single large Hirano body occurs by transport directed towards the minus ends of microtubules as has been shown for formation of aggresomes (Johnston et al., 1998). In addition, it is possible that aberrant function of the actin cytoskeleton generates a signal for formation of Hirano bodies. Studies of such potential mechanisms will be an important goal of future research efforts.

Our studies of live *Dictyostelium* cells containing Hirano bodies are the first studies of the effects of these inclusions on cell physiology, since prior studies have employed fixed material. *Dictyostelium* cells with Hirano bodies grow slowly in suspension, and develop more slowly (Fig. 7) than wild-type cells, but perform phagocytosis and pinocytosis normally. These cells have normal total actin levels, but an increased amount of F-actin, and consequently, a decreased amount of unpolymerized actin compared with wild-type cells. Thus, Hirano bodies may act as a sink for F-actin, sequestering actin and reducing the concentration of free actin available for cellular processes. Thus, the slow growth and slow development phenotypes we observe in CT-myc cells may be due to a reduction in the unpolymerized actin pool. Alternatively, these phenotypes may arise from mechanical hindrance of the ellipsoid and/or disruption of the viscoelastic properties of cytoplasm resulting from CT-myc expression. It is also possible that the presence of a large highly crosslinked ellipsoid may impede processes that require global cytoskeletal changes.

Our findings show clearly that Hirano bodies are not necessarily linked to a stage in cell death. They are toxic neither in *Dictyostelium*, nor in mouse fibroblasts. What then, if any, is the possible significance of Hirano bodies? Actin/cofilin rods are bundles of actin-containing ADF/cofilin that are induced in the cytoplasm following either ATP depletion, oxidative stress (Minamide et al., 2000) or NaCl treatment (Nishida et al., 1987), and in the nucleus following DMSO treatment (Ono et al., 1993) or heat shock (Nishida et al., 1987). These ADF/cofilin actin rods do not reveal the paracrystalline filament organization characteristic of Hirano bodies. Further, ADF/cofilin rods fail to stain with phalloidin, in marked contrast to Hirano bodies, which are strongly labeled both with fluorescent phalloidin and with antibody to cofilin. The change in the twist of the actin filament that results from cofilin-binding explains the reported absence of phalloidin binding to ADF/cofilin rods (McGough et al., 1997). These ADF/cofilin actin rods are associated with >97% of amyloid deposits in brain from Alzheimer's patients, and can form in neurites in cultures resulting in loss of distal microtubules and absence of growth cones (Minamide et al., 2000). These exciting recent results focus attention on aberrant behavior of the actin cytoskeleton as a potentially important feature of loss of cell function in neurodegenerative diseases. Our results show that it cannot be assumed that formation of Hirano bodies is deleterious to cell function. The formation of Hirano bodies may be an adaptive change that promotes cell function. It is possible that the sequestration of actin, cofilin, and other components in Hirano bodies may promote cytoskeletal function by removing them from other regions of the cell. Future studies of actin/cofilin rods and Hirano bodies both in *Dictyostelium* and in mammalian cells may help to elucidate the role(s) of the actin cytoskeleton in the progression of neurodegenerative diseases.

In closing, we propose that formation of Hirano bodies is a general cellular response to or a consequence of aberrant function of the actin cytoskeleton. The unregulated fragment of the 34 kDa protein is the first well-characterized signal shown to induce formation of these assemblies. These findings provide insight into the delicate balance between formation and disassembly of crosslinked actin structures that is necessary for the proper function of the actin cytoskeleton. Actin-binding proteins must be regulated or bind weakly to actin to prevent the accumulation of crosslinked structures. The ability to induce Hirano bodies in cultured cell lines will allow us to explore the mechanism of their formation, and potential adaptive or pathological roles in the various conditions with which they are associated.

We thank Rex Chisholm for supplying the pBORP vector; Richard Meagher, M. Kandasamy, Mary Kimble, Rex Chisholm, Arturo De Lozanne, Catherine Chia, H. Aizawa, Margaret Titus, John Hammer and John Condeelis for generously supplying antibodies as specified in Methods; Francisco Rivero for helpful comments on electroporation of *Dictyostelium*; The Center for Advanced Ultrastructural Research and Mark Farmer for assistance with the electron microscopy and image analysis; Kristen Updegraff for assistance in preparation of the pCT-myc and p34kDa-myc plasmids; and David Eisner and Lindsay Hoskins for help in expression of the CT fragment in mammalian cells. This work was supported by grants from the National Science Foundation (MCB 98-08748) and the Alzheimer's Association.

References

Anzil, A., Herrlinger, H., Blinzinger, K. and Heldrich, A. (1974). Ultrastructure of Brain and Nerve Biopsy tissue in Wilson Disease. *Arch Neurol.* **31**, 94-100.

Atsumi, T., Yamamura, Y., Sato, T. and Ikuta, F. (1980). Hirano bodies in the axon of peripheral nerves in a case with progressive external ophthalmoplegia with multisystemic involvements. *Acta Neuropathol. (Berl.)* **49**, 95-100.

Brier, J., Fechheimer, M., Swanson, J. and Taylor, D. L. (1983). Abundance, relative gelation activity, and distribution of the 95,000 dalton actin-binding protein from *Dictyostelium discoideum*. *J. Cell Biol.* **97**, 178-185.

Buxbaum, J. N. and Tagoe, C. E. (2000). The genetics of the amyloidoses. *Annu. Rev. Med.* **51**, 543-569.

Cano, M. L., Cassimeris, L., Fechheimer, M. and Zigmond, S. H. (1992). Mechanisms responsible for F-actin stabilization after lysis of polymorphonuclear leukocytes. *J. Cell Biol.* **116**, 1123-1134.

Cartier, L., Galvez, S. and Gajdusek, D. C. (1985). Familial clustering of the ataxic form of Creutzfeldt-Jakob disease with Hirano bodies. *J. Neurol. Neurosurg. Psychiatry* **48**, 234-238.

Doering, L. C. and Aguayo, A. J. (1987). Hirano bodies and other cytoskeletal abnormalities develop in fetal rat CNS grafts isolated for long periods in peripheral nerve. *Brain Res.* **401**, 178-184.

Fechheimer, M. (1987). The *Dictyostelium discoideum* 30,000-dalton protein is an actin filament-bundling protein that is selectively present in filopodia. *J. Cell Biol.* **104**, 1539-1551.

Fechheimer, M. and Furukawa, R. (1993). A 27,000 dalton core of the Dictyostelium 34,000 dalton protein retains Ca^{2+}-regulated actin crosslinking but lacks bundling activity. *J. Cell Biol.* **120**, 1169-1176.

Fechheimer, M. and Taylor, D. L. (1984). Isolation and characterization of a 30,000-dalton calcium-sensitive actin crosslinking protein from *Dictyostelium discoideum*. *J. Biol. Chem.* **259**, 4514-4520.

Fechheimer, M. and Zigmond, S. H. (1993). Focusing on unpolymerized actin. *J. Cell Biol.* **123**, 1-5.

Fechheimer, M., Murdock, D., Carney, M. and Glover, C. V. C. (1991). Isolation and sequencing of cDNA clones encoding the *Dictyostelium discoideum* 30,000-dalton actin-bundling protein. *J. Biol. Chem.* **266**, 2883-2889.

Fernandez, R., Fernandez, J. M., Cervera, C., Teijeira, S., Teijeiro, A., Dominguez, C. and Navarro, C. (1999). Adult glycogenosis II with paracrystalline mitochondrial inclusions and Hirano bodies in skeletal muscle. *Neuromuscul. Disord.* **9**, 136-143.

Field, E. J. and Narang, H. K. (1972). An electron-microscopic study of Scrapie in the rat: further observations on 'inclusion bodies' and virus-like particles. *J. Neurol. Sci.* **17**, 347-364.

Field, E. J., Mathews, J. D. and Raine, C. S. (1969). Electron microscopic observations on the cerebellar cortex in kuru. *J. Neurol. Sci.* **8**, 209-224.

Fisher, E. R., Gonzalez, A. R., Khurana, R. C. and Danowski, T. S. (1972). Unique, concentrically laminated, membranous inclusions in myofibers. *Am. J. Clin. Pathol.* **58**, 239-244.

Fu, Y., Ward, J. and Young, H. F. (1975). Unusual, rod-shaped cytoplasmic inclusions (Hirano bodies) in a cerebellar hemangioblastoma. *Acta Neuropathol. (Berl.)* **31**, 129-135.

Furukawa, R. and Fechheimer, M. (1994). Differential localization of alpha-actinin and the 30 kDa actin-bundling protein in the cleavage furrow, phagocytic cup, and contractile vacuole of *Dictyostelium discoideum*. *Cell Motil. Cytoskeleton* **29**, 46-56.

Furukawa, R. and Fechheimer, M. (1997). The structure, function, and assembly of actin filament bundles. *Int. Rev. Cytol.* **175**, 29-90.

Furukawa, R., Butz, S., Fleischmann, E. and Fechheimer, M. (1992). The *Dictyostelium discoideum* 30,000 dalton protein contributes to phagocytosis. *Protoplasma* **169**, 18-27.

Galloway, P. G., Perry, G. and Gambetti, P. (1987). Hirano body filaments contain actin and actin-associated proteins. *J. Neuropathol. Exp. Neurol.* **46**, 185-199.

Galvin, J. E., Lee, V. M., Schmidt, M. L., Tu, P. H., Iwatsubo, T. and Trojanowski, J. Q. (1999). Pathobiology of the Lewy body. *Adv. Neurol.* **80**, 313-324.

Garcia-Mata, R., Bebok, Z., Sorscher, E. J. and Sztul, E. S. (1999). Characterization and dynamics of aggresome formation by a cytosolic-GFP chimera. *J. Cell Biol.* **146**, 1239-1254.

Gessaga, E. C. and Anzil, A. P. (1975). Rod-shaped filamentous inclusions and other ultrastructural features in a cerebellar astrocytoma. *Acta Neuropathol. (Berl.)* **33**, 119-127.

Gibson, P. H. (1978). Light and electron microscopic observations on the relationship between Hirano bodies, neuron and glial perikarya in the human hippocampus. *Acta Neuropathol. (Berl.)* **42**, 165-171.

Gibson, P. H. and Tomlinson, B. E. (1977). Numbers of Hirano bodies in the hippocampus of normal and demented people with Alzheimer's disease. *J. Neurol. Sci.* **33**, 199-206.

Goedert, M. (1999). Filamentous nerve cell inclusions in neurodegenerative diseases: tauopathies and alpha-synucleinopathies. *Philos. Trans. R. Soc. Lond. B Biol. Sci.* **354**, 1101-1118.

Goldman, J. E. (1983). The association of actin with Hirano bodies. *J. Neuropathol. Exp. Neurol.* **42**, 146-152.

Hacker, U., Albrecht, R. and Maniak, M. (1997). Fluid-phase uptake by macropinocytosis in *Dictyostelium*. *J. Cell Sci.* **110**, 105-112.

Hadfield, M. G., Martinez, A. J. and Gilmartin, R. C. (1974). Progressive multifocal leukoencephalopathy with paramyxovirus-like structures, Hirano bodies and neurogibrillary tangles. *Acta. Neuropathol. (Berl.)* **27**, 277-288.

Hirano, A. (1994). Hirano bodies and related neuronal inclusions. *Neuropathol. Appl. Neurobiol.* **20**, 3-11.

Hirano, A., Dembitzer, H. M., Kurland, L. T. and Zimmerman, H. M. (1968). The fine structure of some intraganglionic alterations. *J. Neuropathol. Exp. Neurol.* **27**, 167-182.

Izumiyama, N., Ohtsubo, K., Tachikawa, T. and Nakamura, H. (1991). Elucidation of three-dimensional ultrastructure of Hirano bodies by the quick-freeze, deep-etch and replica method. *Acta Neuropathol. (Berl.)* **81**, 248-254.

Johnston, J. A., Ward, C. L. and Kopito, R. R. (1998). Aggresomes: a cellular response to misfolded proteins. *J. Cell Biol.* **143**, 1883-1898.

Kimble, M., Khodjakov, A. L. and Kuriyama, R. (1992). Identification of ubiquitous high-molecular-mass, heat stable microtubule-associated proteins (MAPs) that are related to the Drosophila 205 kDa MAP but are not related to the Mammalian MAP-4. *Proc. Natl. Acad. Sci. USA* **89**, 7693-7697.

Koo, E. H., Lansbury, P. T. J. and Kelly, J. W. (1999). Amyloid diseases: abnormal protein aggregation in neurodegeneration. *Proc. Natl. Acad. Sci. USA* **96**, 9989-9990.

Lass, R. and Hagel, C. (1994). Hirano bodies and chronic alcoholism. *Neuropath. Appl. Neurobiol.* **20**, 12-21.

Lim, R. W. and Fechheimer, M. (1997). Overexpression, purification, and characterization of recombinant *Dictyostelium discoideum* calcium-regulated 34,000-dalton F-actin bundling protein form *Eschericha coli*. *Protein Expr. Purif.* **9**, 182-190.

Lim, R. W. L., Furukawa, R., Eagle, S., Cartwright, R. C. and Fechheimer, M. (1999a). Three distinct F-actin binding sites in the *Dictyostelium discoideum* 34,000 dalton actin bundling protein. *Biochemistry* **38**, 800-812.

Lim, R. W. L., Furukawa, R. and Fechheimer, M. (1999b). Evidence of intramolecular regulation of the Dictyostelium discoideum 34,000 dalton F-actin bundling protein. *Biochemistry* **38**, 16323-16332.

Loomis, W. F. (1971). Sensitivity of *Dictyostelium discoideum* to nucleic acid analogues. *Exp. Cell Res.* **64**, 484-486.

Lunkes, A., Trottier, Y. and Mandel, J. L. (1998). Pathological mechanisms in Huntington's disease and other polyglutamine diseases. *Essays Biochem.* **33**, 149-163.

Maciver, S. K. and Harrington, C. R. (1995). Two actin binding proteins, actin depolymerizing factor and cofilin, are associated with Hirano bodies. *Neuroreport* **6**, 1985-1988.

Maniak, M., Rauchenberger, R., Albrecht, R., Murphy, J. and Gerisch, G. (1995). Coronin involved in phagocytosis- dynamics of particle-induced relocalization visualized by a green fluorescent protein tag. *Cell* **83**, 915-924.

Mann, S. K. O., Devreotes, P. N., Eliott, S., Jermyn, K., Kuspa, A., Fechheimer, M., Furukawa, R., Parent, C. A., Segall, J., Shaulsky, G. et al. (1998). cell biological, molecular genetic, and biochemical methods to examine *Dictyostelium*. In *Cell Biology: A Laboratory Handbook*, Vol. 1 (ed. J. E. Celis), pp. 431-465. San Diego, CA: Academic Press.

Mattson, M. P. (1997). Cellular actions of β-amyloid precursor protein and its soluble and fibrillogenic derivatives. *Physiol. Rev.* **77**, 1081-1132.

Maupin-Szamier, P. and Pollard, T. D. (1978). Actin filament destruction by osmium tetroxide. *J. Cell Biol.* **77**, 837-852.

McGough, A., Pope, B., Chiu, W. and Weeds, A. (1997). Cofilin changes the twist of F-actin: implications for actin filament dynamics and cellular function. *J. Cell Biol.* **138**, 771-781.

Minamide, L. S., Striegl, A. M., Boyle, J. A., Meberg, P. J. and Bamburg, J. R. (2000). Neurodegenerative stimuli induce persistent ADF/cofilin-actin rods that disrupt distal neurite function. *Nat. Cell Biol.* **2**, 628-636.

Mitake, S., Ojika, K. and Hirano, A. (1997). Hirano bodies and Alzheimer's disease. *Kaohsiung J. Med. Sci.* **13**, 10-18.

Mori, H., Tomonaga, M., Baba, N. and Kanaya, K. (1986). The structure analysis of Hirano bodies by digital processing on electron micrographs. *Acta Neuropathol.* **71**, 32-37.

Nagara, H., Yajima, K. and Suzuki, K. (1980). An ultrastructural study on the cerebellum of the brindled mouse. *Acta Neuropathol. (Berl.)* **52**, 41-50.

Nishida, E., Iida, K. and Yonezawa, N. (1987). Cofilin is a component of intranuclear and cytoplasmic actin rods induced in cultured cells. *Proc. Natl. Acad. Sci. USA* **84**, 5262-5266.

Noegel, A. A. and Schleicher, M. (2000). The actin cytoskeleton of *Dictyostelium*: a story told by mutants. *J. Cell Sci.* **113**, 759-766.

Novak, K. D., Peterson, M. D., Reedy, M. C. and Titus, M. A. (1995). *Dictyostelium* myosin I double mutants exhibit conditional defects in pinocytosis. *J. Cell Biol.* **131**, 1205-1221.

Ogata, J., Budzilovich, G. N. and Cravioto, H. (1972). A study of rod-like structures (Hirano bodies) in 240 normal and pathological brains. *Acta Neuropathol. (Berl.)* **21**, 61-67.

Okamoto, K., Hirai, S. and Hirano, A. (1982). Hirano bodies in myelinated fibers of hepatic encephalopathy. *Acta Neuropathol. (Berl.)* **58**, 307-310.

Ono, S., Abe, H., Nagaoka, R. and Obinata, T. (1993). Colocalization of ADF and cofilin in intranuclear rods of cultured muscle cells. *J. Muscle Res. Cell Motil.* **14**, 195-204.

Ostrow, B. D., Chen, P. X. and Chisholm, R. L. (1994). Expression of a myosin regulatory light-chain phosphorylation site mutant complements the cytokinesis and developmental defects of Dictyostelium RMLC null cells. *J. Cell Biol.* **127**, 1945-1955.

Owen, C. H., Derosier, D. J. and Condeelis, J. (1992). Actin crosslinking protein EF-1α of *Dictyostelium discoideum* has a unique bonding rule that allows square packed bundles. *J. Struct. Biol.* **109**, 248-254.

Papka, M., Rubio, A. and Schiffer, R. B. (1998). A review of Lewy body disease, an emerging concept of cortical dementia. *J. Neuropsychiatry Clin. Neurosci.* **10**, 267-279.

Paulson, H. L. (2000). Toward an understanding of polyglutamine neurodegeneration. *Brain Pathol.* **10**, 293-299.

Peterson, C., Suzuki, K., Kress, Y. and Goldman, J. E. (1986). Abnormalities of dendritic actin organization in the brindled mouse. *Brain Res.* **382**, 205-212.

Rezabek, B. L., Rodriguez-Paris, J. M., Cardelli, J. A. and Chia, C. P. (1997). Phagosomal proteins of *Dictyostelium discoideum*. *J. Euk. Microbiol.* **44**, 284-292.

Rivero, F., Furukawa, R., Noegel, A. A. and Fechheimer, M. (1996). *Dictyostelium discoideum* cells lacking the 34,000 dalton actin binding protein can grow, locomote, and develop, but exhibit defects in regulation of cell structure and movement: a case of partial redundancy. *J. Cell Biol.* **135**, 965-980.

Schmidt, M. L., Lee, V. M. and Trojanowski, J. Q. (1989). Analysis of epitopes shared by Hirano bodies and neurofilament proteins in normal and Alzheimer's disease hippocampus. *Lab Invest.* **60**, 513-522.

Schochet, S. S., Jr, Lampert, P. W. and Lindenberg, R. (1968). Fine structure of the Pick and Hirano bodies in a case of Pick's disease. *Acta Neuropathol. (Berl.)* **11**, 330-337.

Schochet, S. S., Jr and McCormick, W. F. (1972). Ultrastructure of Hirano bodies. *Acta Neuropathol. (Berl.)* **21**, 50-60.

Selkoe, D. J. (1998). The cell biology of β-amyloid precursor protein and presenilin in Alzheimer's disease. *Trends Cell Biol.* **8**, 447-453.

Setoguti, T., Esumi, H. and Shimizu, T. (1974). Specific organization of intracytoplasmic filaments in the dog testicular interstitial cell. *Cell Tissue Res.* **148**, 493-497.

Sima, A. A. and Hinton, D. (1983). Hirano-bodies in the distal symmetric polyneuropathy of the spontaneously diabetic BB-Wistar rat. *Acta Neurol. Scand.* **68**, 107-112.

Tilney, L. G. and Tilney, M. S. (1994). Methods to Visualize actin polymerization associated with bacterial invasion. *Methods Enzymol.* **236**, 476-481.

Tolnay, M. and Probst, A. (1999). Tau protein pathology in Alzheimer's disease and related disorders. *Neuropathol. Appl. Neurobiol.* **25**, 171-187.

Tomonaga, M. (1974). Ultrastructure of Hirano bodies. *Acta Neuropathol. (Berl.)* **28**, 365-366.

Tomonaga, M. (1983). Hirano body in extraocular muscle. *Acta Neuropathol. (Berl.)* **60**, 309-313.

Waggoner, D. J., Bartnikas, T. B. and Gitlin, J. D. (1999). The role of copper in neurodegenerative disease. *Neurobiol. Dis.* **6**, 221-230.

Wigley, W. C., Fabunmi, R. P., Lee, M. G., Marino, C. R., Muallem, S., DeMartino, G. N. and Thomas, P. J. (1999). Dynamic association of the proteasomal machinery with the centrosome. *J. Cell Biol.* **145**, 481-490.

Yagishita, S., Itoh, Y., Nakano, T., Ono, Y. and Amano, N. (1979). Crystalloid inclusions reminiscent of Hirano bodies in autolyzed peripheral nerve of normal wistar rats. *Acta Neuropathol (Berl.)* **47**, 231-236.

Yamamoto, T. and Hirano, A. (1985). Hirano bodies in the perikaryon of the Purkinje cell in a case of Alzheimer's disease. *Acta Neuropathol. (Berl.)* **67**, 167-169.

Zigmond, S. H., Furukawa, A. and Fechheimer, M. (1992). Inhibition of actin filament depolymerization by the *Dictyostelium* 30,000 dalton actin-bundling protein. *J. Cell Biol.* **119**, 559-567.